An Efficient Algorithm for Simulating the Real-Time Quantum Dynamics of a Single Spin-1/2 Coupled to Specific Spin-1/2 Baths

2012 J. Phys.: Conf. Ser. 402 012019

(http://iopscience.iop.org/1742-6596/402/1/012019)

Journal of Physics: Conference Series **402** (2012) 012019 doi:10.1088/1742-6596/402/1/012019

An Efficient Algorithm for Simulating the Real-Time Quantum Dynamics of a Single Spin-1/2 Coupled to Specific Spin-1/2 Baths

M A Novotny[1,2,5], M Guerra[1,2,3], H De Raedt[4], K Michielsen[5,6], F Jin[5]

[1] Department of Physics and Astronomy, Mississippi State University, Mississippi State, MS 39762-5167, USA
[2] HPC[2] Center for Computational Sciences, Mississippi State University, Mississippi State, MS 39762-5167, USA
[3] Department of Sciences & Mathematics, Mississippi University for Women, 1100 College Street, MUW-100, Columbus, MS 39701, USA
[4] Department of Applied Physics, Zernike Institute of Advanced Materials, University of Groningen, Nijenborgh 4, NL-9747 AG Groningen, The Netherlands
[5] Institute for Advanced Simulation, Jülich Supercomputing Centre, Forschungszentrum Jülich, D-52425 Jülich, Germany
[6] RWTH Aachen University, D-52056 Aachen, Germany

E-mail: man40@ra.msstate.edu

Abstract. An efficient algorithm for the computation of the real-time dependence of a single quantum spin-1/2 coupled to a specific set of quantum spin-1/2 baths is presented. The specific spin baths have couplings only with the spin operators S^x between bath spins and the central spin. We calculate spin expectation values, the quantum purity, the von Neumann entropy, and the off-diagonal components of the reduced density matrix for the central spin once the bath spins have been traced out. The algorithm does not require the storage of any vector larger than of size 2, even though the size of the Hilbert space is 2^{N+1}, where N is the number of bath spins. Results are presented for the central spin connected to different sizes and types of spin baths, and for different initial states for the central spin and for the bath spins. Results are also compared to those for more general baths.

1. Introduction

The real-time (as opposed to imaginary time) quantum dynamics of systems is becoming more and more of interest. This interest is driven by the increasingly precise experiments that are being performed on quantum systems, and by the long-range goal of building a quantum computer [1, 2]. The calculation that needs to be performed is to solve the time-dependent Schödinger equation (TDSE) [3]

$$\mathcal{H}\,|\Psi(t)\rangle = -\frac{\hbar}{i}\frac{\partial}{\partial t}\,|\Psi(t)\rangle\,, \tag{1}$$

where the Hamiltonian $\mathcal{H}$ is assumed to be independent of time and the initial state $|\Psi(0)\rangle$ is given. Furthermore, if the closed quantum system is thought of as being composed of a

subsystem S and an environment or bath B, then the Hamiltonian can be written as

$$\mathcal{H} = \mathcal{H}_S + \mathcal{H}_B + \mathcal{H}_{SB}, \tag{2}$$

with the first term the Hamiltonian describing the subsystem S, the second term describes the Hamiltonian of the bath B, and the third term the Hamiltonian describing the coupling between the subsystem S and the bath B. Spin baths have been studied since at least the time of Fermi [4], and are also of recent interest [5, 6, 7]. In this paper we assume that the subsystem S consists of one spin-1/2 particle, also called the central spin, and that the bath B is composed of N spin-1/2 particles. The dimension of the Hilbert space for the bath is $D_B = 2^N$ and the dimension of the complete Hilbert space is $2D_B = 2^{N+1}$. The dimension of the vector $|\Psi(t)\rangle$ in Eq. (1) is 2^{N+1}. The state of the subsystem S is described by the reduced density matrix

$$\rho(t) = \mathrm{Tr}_B \left[\rho_{S+B}(t)\right], \tag{3}$$

where ρ_{S+B} is the density matrix of the complete $N+1$ spin system, and the trace is over the N spins in the bath. Thus $\rho(t)$ is a 2×2 matrix. However, to calculate $\rho(t)$ one first needs to propagate the state

$$|\Psi(t)\rangle = \exp\left(-\frac{i\mathcal{H}t}{\hbar}\right)|\Psi(0)\rangle, \tag{4}$$

for all $N+1$ spins according to the TDSE, and then trace out the bath spins.

The dimension of $|\Psi(t)\rangle$ presents a large difficulty in computer calculations of spin systems. We want to have N large, but memory of computers is limited. For example, the most powerful computer in the world on the November 2011 Top 500 list [8], the K computer at the RIKEN Advanced Institute for Computational Science in Japan, has 705,024 cores and operates at 10.5 Petaflop/s on the Linpack benchmark. Each compute node of the K computer has 16 Gbyte of memory, so the memory of the K computer is about 1.2×10^{16} bytes, which means that the number of spins for the largest vector $|\Psi(t)\rangle$ that can be stored in the K computer is about $N \approx 50$. Even the stated goal for exascale computing that the memory should be on the order of a few exabytes, limits the size of the vector $|\Psi(t)\rangle$ to about $N \approx 60$.

Clearly, algorithmic advances that could increase N without requiring storage of vectors of size 2^{N+1} would be extremely advantageous. In this article we present such an algorithm, where the only storage required is of vectors of size 2. This algorithm works only for specific types of baths. Although the type of bath can be generalized, in this paper we concentrate on one type of bath, which we call an x-bath, detailed explicitly in the next section. This type of bath can also be used for more than one spin in the subsystem of interest, but in order to describe the algorithm and explore the efficiency of this type of bath we limit ourselves to a single central spin. We assume that an efficient algorithm to calculate the TDSE for any Hamiltonian is available, such as the efficient method based on Chebyshev polynomials [9, 10, 11, 12]. We also present results for more general baths using the Chebyshev algorithm [12], comparing with our x-bath results. A recent paper reported the use of up to 36 spin-1/2 particles to study decoherence and thermalization [13] storing the full vectors of size 2^{36} required for the computations. The number of spins that can be included in computer calculations is small compared to the size of spin baths in laboratory experiments. For example, recent experiments studied a single electron coupled to a bath of about 10^9 spins [14, 15].

2. Methodology

We consider a single spin-1/2 particle coupled to a quantum bath of N spin-1/2 particles. The dimension of the Hilbert space is 2^{N+1}. Let the central spin be numbered spin 0, and the x-bath spins 1 through N. The Pauli spin matrices σ^x, σ^y, and σ^z are given by

$$s^x = \frac{\hbar}{2}\sigma^x = \frac{\hbar}{2}\begin{pmatrix} 0 & 1 \\ 1 & 0 \end{pmatrix}, \quad s^y = \frac{\hbar}{2}\sigma^y = \frac{\hbar}{2}\begin{pmatrix} 0 & -i \\ i & 0 \end{pmatrix}, \quad s^z = \frac{\hbar}{2}\sigma^z = \frac{\hbar}{2}\begin{pmatrix} 1 & 0 \\ 0 & -1 \end{pmatrix}. \tag{5}$$

We define

$$S_m^\ell = I_2 \otimes I_2 \otimes \cdots \otimes I_2 \otimes s^\ell \otimes I_2 \otimes \cdots \otimes I_2, \tag{6}$$

with I_2 the 2×2 identity matrix and s^ℓ the 2×2 Pauli spin matrix ($\ell \in \{x, y, z\}$) at the m^{th} position in the Kronecker (direct) product of $N+1$ matrices of size 2×2. Here $m \in \{0, \cdots, N\}$ with $m = 0$ referring to the central spin and $m \in \{1, \cdots, N\}$ referring to the bath spins.

From now on we set $\hbar = 1$. The system Hamiltonian that we consider contains the following terms

$$\mathcal{H}_S = \omega_0 S_0^z, \tag{7}$$

where ω_0 denotes the strength of the external magnetic field that is applied to the central spin in the z-direction,

$$\mathcal{H}_B = \sum_{i_1=0}^{1} \sum_{i_2=0}^{1} \cdots \sum_{i_N=0}^{1} \widetilde{J}_{i_1,i_2,\cdots,i_N} \left(S_1^x\right)^{i_1} \left(S_2^x\right)^{i_2} \cdots \left(S_N^x\right)^{i_N} \ , \tag{8}$$

where $\widetilde{J}_{i_1,i_2,\cdots,i_N}$ denotes the strength of the coupling between the N spins in the x-bath. Furthermore, we assume that

$$\mathcal{H}_{SB} = S_0^x \left[\sum_{i_1=0}^{1} \sum_{i_2=0}^{1} \cdots \sum_{i_N=0}^{1} J_{i_1,i_2,\cdots,i_N} \left(S_1^x\right)^{i_1} \left(S_2^x\right)^{i_2} \cdots \left(S_N^x\right)^{i_N} \right] \tag{9}$$

where $J_{i_1,i_2,\cdots,i_N}$ denotes the strength of the coupling between the central spin and the N spins in the x-bath. Note that the type of spin interaction (2-spin, 3-spin, $\cdots$) is specified by the number of ones in the subscript of J or $\widetilde{J}$ since it follows from Eq. (6) that $\left(S_i^x\right)^0 = I_{\text{F}}$ where I_F denotes the $2^{N+1} \times 2^{N+1}$ identity matrix. For later, we define J_2 (J_3) as the strength of the two(three)-body interactions between the central spin and a (couple of) bath spin(s) in the case that they are all equal. Similarly, J_M denotes the strength of the N-body interactions between the central spin and the $N-1$ tuples of bath spins (only one bath spin is not in the sum) times 2^N, again for the case that the respective interactions are all equal. In addition, J_A denotes 2^{N+1} times the strength of the $(N+1)$-body interactions between the central spin and all bath spins. (The additional factors of 2 in the definitions of J_M and J_A are present for convenience. They are inserted because of the factor of $1/2$ in $s^\ell = \sigma^\ell/2$. No factors of 2 are present in our definitions of J_2 or J_3.)

We first introduce the matrix

$$p_x = \frac{1}{\sqrt{2}} \begin{pmatrix} 1 & -1 \\ 1 & 1 \end{pmatrix} , \tag{10}$$

having the properties $p_x p_x^{-1} = I_2$ with $p_x^{-1} = p_x^{\text{T}} = p_x^\dagger$. The matrix p_x also exhibits the property $p_x^\dagger s^x p_x = s^z$. In addition

$$p_x^\dagger \begin{pmatrix} 0 \\ 1 \end{pmatrix} = \frac{1}{\sqrt{2}} \begin{pmatrix} 1 \\ 1 \end{pmatrix} . \tag{11}$$

We next introduce the matrix

$$P_p = I_2 \otimes p_x \otimes p_x \otimes \cdots p_x \ , \tag{12}$$

with the position 0 in the Kronecker product the 2×2 identity matrix I_2 and the positions 1 through N in the Kronecker product occupied by p_x. It follows that $P_p^\dagger P_p = I_F$, where I_F

denotes the $2^{N+1} \times 2^{N+1}$ identity matrix. By performing a unitary transformation with P_p, we obtain the transformed Hamiltonian

$$\begin{aligned}\widetilde{\mathcal{H}} &= P_p^\dagger \mathcal{H} P_p \\ &= \omega_0 S_0^z + \sum_{i_1=0}^{1}\sum_{i_2=0}^{1}\cdots\sum_{i_N=0}^{1} \widetilde{J}_{i_1,i_2,\cdots,i_N} \left(S_1^z\right)^{i_1}\left(S_2^z\right)^{i_2}\cdots\left(S_N^z\right)^{i_N} \\ &\quad + S_0^x\left[\sum_{i_1=0}^{1}\sum_{i_2=0}^{1}\cdots\sum_{i_N=0}^{1} J_{i_1,i_2,\cdots,i_N} \left(S_1^z\right)^{i_1}\left(S_2^z\right)^{i_2}\cdots\left(S_N^z\right)^{i_N}\right] . \end{aligned} \tag{13}$$

Thus the Hamiltonian $\widetilde{\mathcal{H}}$ is block diagonal with 2^N blocks of 2×2 matrices labeled by the index j and all having the form

$$\widetilde{\mathcal{H}}_j = \begin{pmatrix} \Omega_{zj}+\omega_0 & \Omega_{xj} \\ \Omega_{xj} & \Omega_{zj}-\omega_0 \end{pmatrix} = \Omega_{zj} I_2 + 2\vec{\Omega}_j\cdot\vec{s}, \tag{14}$$

with the vector $\vec{\Omega}_j$ having the components $(\Omega_{xj},\, 0,\, \omega_0)$ and $\left|\vec{\Omega}_j\right| = \sqrt{\Omega_{xj}^2+\omega_0^2}$. The eigenvalues of $\widetilde{\mathcal{H}}_j$ are$\Omega_{zj} \pm \left|\vec{\Omega}_j\right|$. Note that Ω_{zj} depends on the $\widetilde{J}$ couplings only, and thatΩ_{xj} depends only on the J couplings. The Hamiltonian $\widetilde{H}$ can thus also be written as

$$\widetilde{\mathcal{H}} = \widetilde{\mathcal{H}}_1 \oplus \widetilde{\mathcal{H}}_2 \oplus \cdots \oplus \widetilde{\mathcal{H}}_{2^N} . \tag{15}$$

As in [13] we assume that the central spin is decoupled from the bath for times $t<0$, and that the central spin and the bath spins are brought into contact at time $t=0$. We assume that at time $t=0$ the central spin is in the state

$$|\psi(0)\rangle = \begin{pmatrix} \sin\alpha_0 \\ \cos\alpha_0 \end{pmatrix} \tag{16}$$

so that if $\alpha_0 = 0$ the central spin starts in the down state, and it starts in the up state for $\alpha_0 = \frac{\pi}{2}$. Note that the unitary transformation in Eq. (12) does not change the initial state of the central spin at time $t=0$. After the unitary transformation by P_p at time $t=0$ the state of the bath can be written as

$$\left|\widetilde{\Phi}(0)\right\rangle = \sum_{j=1}^{2^N} c_j \left|\varphi_j\right\rangle \qquad \text{with} \qquad \sum_{j=1}^{2^N} |c_j|^2 = 1, \tag{17}$$

with some complex coefficients c_j and $\{|\varphi_j\rangle\}$ the complete orthonormal set of states taken to be the usual direct products of the spin up and down states of the N bath spins. In practice one can regard the c_j as the coefficients obtained after starting with the $t=0$ bath state $|\Phi(0)\rangle$ in the orthonormal basis of the eigenvectors of σ^x for the x-bath spins, which with the unitary transformation by $P_p^\dagger$ gives the environment spin state of Eq. (17).

The expectation values $\langle S_0^\ell(t)\rangle$ are independent of the values of $\widetilde{J}_{i_1,i_2,\cdots,i_N}$. With the initial state $|\Psi(0)\rangle = |\psi(0)\rangle\otimes|\Phi(0)\rangle$ this independence is because these terms only enter inΩ_{zj}, and furthermore,

$$\begin{aligned}\left\langle S_0^\ell(t)\right\rangle &= \langle\Psi(0)|\exp\left(i\mathcal{H}t\right)\left(s^\ell\otimes I_2\otimes I_2\otimes\cdots\otimes I_2\right)\exp\left(-i\mathcal{H}t\right)|\Psi(0)\rangle \\ &= \left\langle\widetilde{\Psi}(0)\right|\exp\left(i\widetilde{\mathcal{H}}t\right)\left(s^\ell\otimes I_2\otimes I_2\otimes\cdots\otimes I_2\right)\exp\left(-i\widetilde{\mathcal{H}}t\right)\left|\widetilde{\Psi}(0)\right\rangle , \end{aligned} \tag{18}$$

with $\left|\widetilde{\Psi}(0)\right\rangle = P_p^\dagger \left|\Psi(0)\right\rangle$. The reason is that

$$\mathcal{H} = P_p \widetilde{\mathcal{H}} P_p^\dagger, \quad \text{so} \quad \exp\left[i\mathcal{H}t\right] = P_p \exp\left[i\widetilde{\mathcal{H}}t\right] P_p^\dagger \,, \tag{19}$$

and the constant termsΩ_{zj} in each block cancel because they commute with everything. One Ω_{zj} term comes from each of the blocks $\widetilde{H}$ in Eq. (19), and $\exp\left[i\Omega_{zj}t\right]\exp\left[-i\Omega_{zj}t\right] = 1$.

Next we want to trace out the bath spins to be left with the density matrix $\rho(t)$ for the central spin. At $t = 0$ the density matrix of the central spin is

$$\rho(0) = \left|\psi(0)\right\rangle\left\langle\psi(0)\right| \,. \tag{20}$$

Explicitly

$$\begin{aligned}
\rho(t) &= \mathrm{Tr}_B\left[e^{-i\mathcal{H}t}\left(\rho(0)\otimes\rho_B(0)\right)e^{i\mathcal{H}t}\right] &(21)\\
&= \mathrm{Tr}_B\left[P_p e^{-i\widetilde{\mathcal{H}}t} P_p^\dagger \left(\rho(0)\otimes\rho_B(0)\right) P_p e^{i\widetilde{\mathcal{H}}t} P_p^\dagger\right] &(22)\\
&= \mathrm{Tr}_B\left[e^{-i\widetilde{\mathcal{H}}t}\left(\rho(0)\otimes\widetilde{\rho}_B(0)\right)e^{i\widetilde{\mathcal{H}}t}\right] \,. &(23)
\end{aligned}$$

Here $\widetilde{\rho}_B(0) = \left|\widetilde{\Phi}(0)\right\rangle\left\langle\widetilde{\Phi}(0)\right|$. Writing Eq. (23) in terms of the c_j of Eq. (17) and the block diagonal matrices $\mathcal{H}_j$ of Eq. (14) gives the final equation for the reduced density matrix for the central spin,

$$\begin{aligned}
\rho(t) &= \left(\left|c_1\right|^2 e^{-i\widetilde{\mathcal{H}}_1 t}\rho(0)e^{i\widetilde{\mathcal{H}}_1 t}\right) + \left(\left|c_2\right|^2 e^{-i\widetilde{\mathcal{H}}_2 t}\rho(0)e^{i\widetilde{\mathcal{H}}_2 t}\right) + \cdots + \left(\left|c_{2^N}\right|^2 e^{-i\widetilde{\mathcal{H}}_{2^N} t}\rho(0)e^{i\widetilde{\mathcal{H}}_{2^N} t}\right)\\
&= \left|c_1\right|^2\rho_1(t) + \left|c_2\right|^2\rho_2(t) + \cdots + \left|c_{2^N}\right|^2\rho_{2^N}(t) \,. &(24)
\end{aligned}$$

Equation (24) shows that the reduced quantum density matrix $\rho(t)$ for the central spin is the sum of 2^N different 2×2 density matrices $\rho_j(t)$. Notice that the initial state of the bath spins enters only in the terms $\left|c_j\right|^2$. The 2×2 matrix exponentials can easily be calculated using the relation

$$\exp\left[\pm i\left(\vec{a}\cdot\vec{\sigma}\right)t\right] \;=\; I_2\cos\left(at\right) \pm i\frac{\vec{a}\cdot\vec{\sigma}}{a}\sin\left(at\right) \,, \tag{25}$$

with $a = \left|\vec{a}\right|$.

For any expectation value of the central spin, Eq. (24) gives

$$\left\langle S_0^\ell(t)\right\rangle = \sum_{j=1}^{2^N}\left|c_j\right|^2 \mathrm{Tr}\left[s^\ell\rho_j(t)\right] \,. \tag{26}$$

Thus the final result is that for the type of Hamiltonian defined in Eq. (13) (one connected to an x-bath) the time dependence of the expectation value for any spin operator reduces to the sum over the expectation values of 2^N evolution equations with different Hamiltonians $\widetilde{\mathcal{H}}_j$. Equations (24) and (26) are the central results that will be exploited for our efficient algorithm. Note in particular that only 2×2 matrices must be worked with, and hence stored in memory. However, computationally we do not get something for nothing, in that we have to solve the TDSE for 2^N different Hamiltonians $\widetilde{\mathcal{H}}_j$ and then sum to get the final expectation value.

3. Measured Quantities

We are particularly interested in measuring four types of quantities. The first are the time-dependent expectation values of the central spin, given by Eq. (26).

The second quantity of interest is the quantum purity for the central spin,

$$\mathcal{P}(t) = \mathrm{Tr}\left[\rho(t)^2\right] . \tag{27}$$

Because $\rho(t)$ is a 2×2 matrix we can write it as

$$\rho(t) = a_\rho(t) I_2 + \vec{b}_\rho(t) \cdot \vec{\sigma} \tag{28}$$

with the vector $\vec{b}_\rho(t)$ having components $(b_{\rho x}(t), b_{\rho y}(t), b_{\rho z}(t))$ and $b_\rho(t) = \sqrt{b_{\rho x}^2(t) + b_{\rho y}^2(t) + b_{\rho z}^2(t)}$. Using $\left[\vec{b}_\rho(t) \cdot \vec{\sigma}\right]^2 = b_\rho^2(t) I_2$ gives

$$\mathcal{P}(t) = 2a_\rho^2(t) + 2b_\rho^2(t) . \tag{29}$$

The third quantity of interest is the von Neumann entropy

$$\mathcal{S}(t) = -k_B \mathrm{Tr}\left[\rho(t) \log_2 \rho(t)\right] , \tag{30}$$

where from now on we also set Boltzmann's constant $k_B = 1$. The eigenvalues of $\rho(t)$ are

$$\lambda_\pm(t) = a_\rho(t) \pm b_\rho(t), \tag{31}$$

so that

$$\mathcal{S}(t) = -\lambda_+(t) \log_2\left[\lambda_+(t)\right] - \lambda_-(t) \log_2\left[\lambda_-(t)\right] . \tag{32}$$

The fourth quantity of interest, as defined in Ref. [13], is the sum of the off-diagonal elements of $\rho(t)$

$$\sigma(t) = \sqrt{\sum_{i=1}^{2^{N_s}-1} \sum_{j=i+1}^{2^{N_s}} |\rho_{ij}(t)|^2} , \tag{33}$$

if there were N_s spins in the subsystem. Note $\sigma(t)$ should not be confused with the Pauli spin matrices σ^ℓ. For general N_s, in order for the subsystem to thermalize toward a canonical distribution a necessary condition is that $\sigma(t)$ become very small [13]. In our case $N_s = 1$ so that

$$\sigma(t) = |\rho_{12}(t)| . \tag{34}$$

Since none of these measured quantities depend on the $\widetilde{J}$ couplings, without loss of generality we set all $\widetilde{J} = 0$.

4. Symmetry in interactions with the x-bath spins

Equations (24) and (26) are the central results, and are very general. For the general case where all J values are different one has to sum over 2^N different density matrices $\rho_j(t)$ to obtain $\rho(t)$. If there is any symmetry in the couplings between the central spin and the x-bath spins, then this symmetry can be exploited to reduce the number of terms that must be summed. The reduction comes because the symmetry in the Hamiltonian can make a number of the $\rho_j(t)$ identical. As long as some of the $\rho_j(t)$ are identical, the initial state of the bath need not have any symmetry

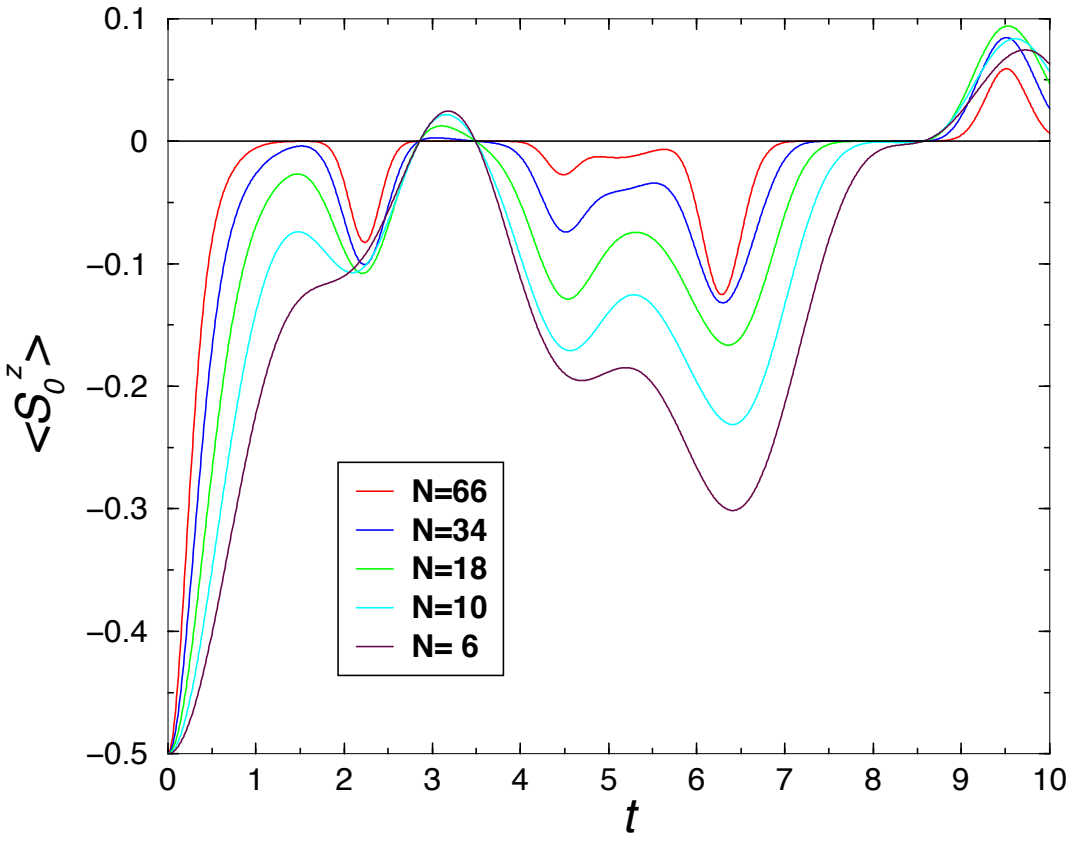

Figure 1. The central spin expectation value $\langle S_0^z(t)\rangle$ as a function of t is shown for different numbers of bath spins N. The N bath spins are divided into two equal baths with $N_1 = N_2 = N/2$. One bath has $J_2 = 0.9$ and $J_M = 0.1$, while the other bath has $J_2 = 1.1$ and $J_M = -0.1$. All spins start initially with spin down. Reading from top to bottom near $t = 0$ the values of N are 66, 34, 18, 10, and 6.

in order to combine terms in the sum of Eqs. (24) or (26). For example, if all $\rho_j(t)$ are identical for $j \in \{i, \cdots, i+k\}$ then in Eq. (26) one can group together the terms that enter the sum to be

$$\left\langle S_0^\ell(t)\right\rangle = \cdots + \left\{ \left(\sum_{j=i}^{i+k} |c_j|^2 \right) \mathrm{Tr}\left[s^\ell \rho_{\mathrm{sym}}(t) \right] \right\} + \cdots \tag{35}$$

with the definition $\rho_j(t) = \rho_{\mathrm{sym}}(t)$ for $j \in \{i, \cdots, i+k\}$. Therefore in this example one only has to solve the TDSE for one block Hamiltonian, rather than for k different block Hamiltonians.

Consider the special case of only two-body interactions between the central spin and the x-bath spins, all with the same coupling J_2. The Hamiltonian of the system (with $\widetilde{J} = 0$), after the unitary transformation with P_p, reads

$$\widetilde{\mathcal{H}}_j \;=\; \omega_0 S_0^z + J_2 S_0^x \left[\sum_{i=1}^{N} S_i^z \right]_j \;=\; \vec{S}_0 \cdot \vec{\Omega}_j \,, \tag{36}$$

where we have defined the vector

$$\vec{\Omega}_j \;=\; \left(J_2 \left[\sum_{i=1}^{N} S_i^z \right]_j ,\; 0,\; \omega_0 \right) . \tag{37}$$

We now make one additional assumption in order to compare directly with the results presented in a recent paper by Rao *et al.* [16]. We assume that the initial state of all the spins (the central spin and all bath spins) is the down state, $|\Psi(0)\rangle = |\psi(0)\rangle \otimes |\Phi(0)\rangle = |\downarrow\downarrow \cdots \downarrow\rangle$. After the transformation with P_p this makes all the $|c_j|^2$ equally probable, so $|c_j|^2 = 2^{-N}$. Then we can organize the sum over the 2^N x-bath spins into ones that are identical, namely classified by the projection m onto the z-axis of the N spins (classified by the magnetization m). There are

$$\lambda_{N,m} = \left(\begin{array}{c} N \\ N/2-m \end{array} \right) = \frac{N!}{(N/2-m)!\,(N/2+m)!}, \tag{38}$$

identical vectors $\vec{\Omega}_m = (mJ_2,\, 0,\, \omega_0)$ where $-N/2 \le m \le N/2$ with m having integer steps. The Hamiltonian of each 2×2 block has the form as given in Eq. (14), which here is explicitly

$$\mathcal{H}_m = \left(\begin{array}{cc} \omega_0 & mJ_2 \\ mJ_2 & -\omega_0 \end{array} \right) . \tag{39}$$

The result for $\langle S_0^z(t)\rangle$ is thus the sum not over 2^N terms but of only $N+1$ terms that have the form, with$\Omega_{xm} = mJ_2$,

$$\left(\begin{array}{cc} 0 & 1 \end{array} \right) \exp\left[i\widetilde{\mathcal{H}}_m t \right] \frac{1}{2} \left(\begin{array}{cc} 1 & 0 \\ 0 & -1 \end{array} \right) \exp\left[-i\widetilde{\mathcal{H}}_m t \right] \left(\begin{array}{c} 0 \\ 1 \end{array} \right) = \frac{1}{2} \frac{\omega_0^2 + \Omega_{xm}^2 \cos\left[\sqrt{\Omega_{xm}^2 + \omega_0^2}\, t \right]}{\Omega_{xm}^2 + \omega_0^2}. \tag{40}$$

Note that if $m = 0$ then $\Omega_{xm} = mJ_2 = 0$, and if the applied field $\omega_0 = 0$ the term in Eq. (40) equals $-1/2$. Since $\alpha_0 = 0$ the initial central spin density matrix is

$$\rho(0) = |\downarrow\rangle \langle\downarrow| = \left(\begin{array}{c} 0 \\ 1 \end{array} \right) \left(\begin{array}{cc} 0 & 1 \end{array} \right) = \left(\begin{array}{cc} 0 & 0 \\ 0 & 1 \end{array} \right) . \tag{41}$$

Since we have defined $\vec{\Omega}_m = (mJ_2, 0, \omega_0)$,$\Omega_m = \sqrt{m^2 J_2^2 + \omega_0^2}$. Then the result for the expectation value of the central spin is

$$\langle S_0^z(t)\rangle = \frac{1}{2^{N+1}} \sum_{m=-N/2}^{N/2} \lambda_{N,m} \frac{\left[m^2 J_2^2 \cos\left(\Omega_m t\right) \right] + \omega_0^2}{\Omega_m^2} . \tag{42}$$

As in reference [16], the quantum purity $\mathcal{P}(t)$ for our case is given by

$$\mathcal{P}(t) = \frac{1}{2} \exp\left(-\frac{N J_2^2 t^2}{4} \right) + \frac{1}{2} . \tag{43}$$

Thus, in the absence of disorder in the values of J_2, the quantity $2\mathcal{P}(t) - 1$ decays to its asymptotic value exponentially in $NJ_2^2 t^2$ for one x-bath. We will test whether this is true also when there is disorder in the couplings J_2 of the 2-body interactions with the central spin.

The results can be generalized to the case where there are two x-baths that have only 2-body interactions with the central spin. Explicitly, we consider N_1 x-bath spins with coupling J_2 and N_2 x-bath spins with coupling J_2' with $N = N_1 + N_2$. Then rather than summing over

2^N different terms to find $\rho(t)$, symmetry allows us to sum only over $(N_1+1)(N_2+1)$ terms. Explicitly, one has

$$\langle S_0^z(t)\rangle = \frac{1}{2^{N+1}} \sum_{m_1=-N_1/2}^{N_1/2} \sum_{m_2=-N_2/2}^{N_2/2} \lambda_{N_1,m_1}\lambda_{N_2,m_2} \frac{\left[(m_1J_2+m_2J_2')^2\cos\left(\Omega_{m_1m_2}t\right)\right]+\omega_0^2}{\Omega_{m_1m_2}^2} \quad (44)$$

with the definition $\vec{\Omega}_{m_1m_2} = (m_1J_2+m_2J_2',\ 0,\ \omega_0)$. Of course this relation can be generalized so with different J_2 couplings between the central spin and n different sets of bath spins there would be a sum over $(N_1+1)\,(N_2+1)\cdots(N_n+1)$ different terms rather than $2^N = 2^{N_1+N_2+\cdots+N_n}$ terms.

The results of Eqs. (42) and (44) also can be generalized for the cases when there are more than 2-body couplings between the central spin and the spins in a bath. As long as the interactions are symmetric under the exchange of the label of any two spins in a given bath, again this reduces to a sum over $(N_1+1)\,(N_2+1)\cdots(N_n+1)$ different terms rather than $2^N = 2^{N_1+N_2+\cdots+N_n}$ terms. For example, Eq. (42) holds when all N different couplings between the central spin and the bath spins have the same strength J_2. If all N different N-body couplings had the same strength J_M the symmetry would again hold. The symmetry also holds if there is a $N+1$-body coupling J_A (the central spin is coupled to all N bath spins). If all possible $N(N-1)/2$ 3-body interactions had strength J_3 then the same symmetry holds. Therefore, for any values of J, if the symmetry of relabeling any two spins in every bath holds, then there is only a need to sum over $(N_1+1)\,(N_2+1)\cdots(N_n+1)$ terms.

Use of this symmetry allows calculations for $\langle S_0^\ell\rangle$. In Fig. 1 results are shown for $\langle S_0^z\rangle$, with $N_1 = N_2 = N/2$. One bath has $J_2 = 0.9$ and $J_M = 0.1$ while the other has $J_2' = 1.1$ and $J_M' = -0.1$. The values of N were chosen such that the N_1- and N_2-body interactions have an even number of spins so that $\langle S_0^x\rangle$ is always zero since we start with all spins down. The results in Fig. 1 for $N \le 34$ could be obtained on today's computers using methods such as those described in references [9, 10, 11, 12, 13], because the size of the 2^{N+1} vector that needs to be stored in computer memory is only $2^{35} \approx 3\times10^{10}$. However, the $N = 66$ result in Fig. 1 would require storage of a vector of $2^{67} \approx 1.5\times10^{20}$ words, or about 150 exawords. The stated goal for exascale computing is that the memory should be on the order of a few exabytes, so even the next generation of supercomputers could not perform the $N = 66$ calculations of Fig. 1 using general methods. Furthermore, without use of the symmetry, for the $N = 66$ data of Fig. 1 one would have to sum over $2^{66} \approx 7\times10^{19}$ different 2×2 matrices $\rho_j(t)$ to obtain $\rho(t)$. With the symmetry there are only $67^2 = 4489$ different $\rho_j(t)$ values over which the sum is performed. With the algorithm described in this paper obviously calculations for large N values can be performed. For large values of N the limitation on N may be due to the precision of the computer calculations, rather than due to limitations in computer run time or in computer memory. For example, the next bath size in the sequence of Fig. 1 would be $N = 130$, but using double precision the quantity $2\mathcal{P}(t)-1$ becomes negative due to rounding errors after a time of about $t = 1.1$, while this quantity cannot ever be negative.

The reduction in the number of terms to sum to get $\rho(t)$ only requires symmetry in the Hamiltonian $\mathcal{H}$, not in the initial bath vector $\left|\widetilde{\Phi}(0)\right\rangle$ [see Eqs. (17) and (35)]. If $\mathcal{H}$ has the symmetry, then each term of the sum in Eqs. (42) or (44) is the sum over all the $|c_j|^2$ that have magnetization m. In other words, the replacement (assuming that the initial state is a direct product of the vectors for the N_n baths) just requires the replacement

$$\frac{1}{2^{N_j}}\,\lambda_{N_j,m_j} \longleftrightarrow \sum_{i=1}^{2^N}{}' \left|c_i\right|^2 , \quad (45)$$

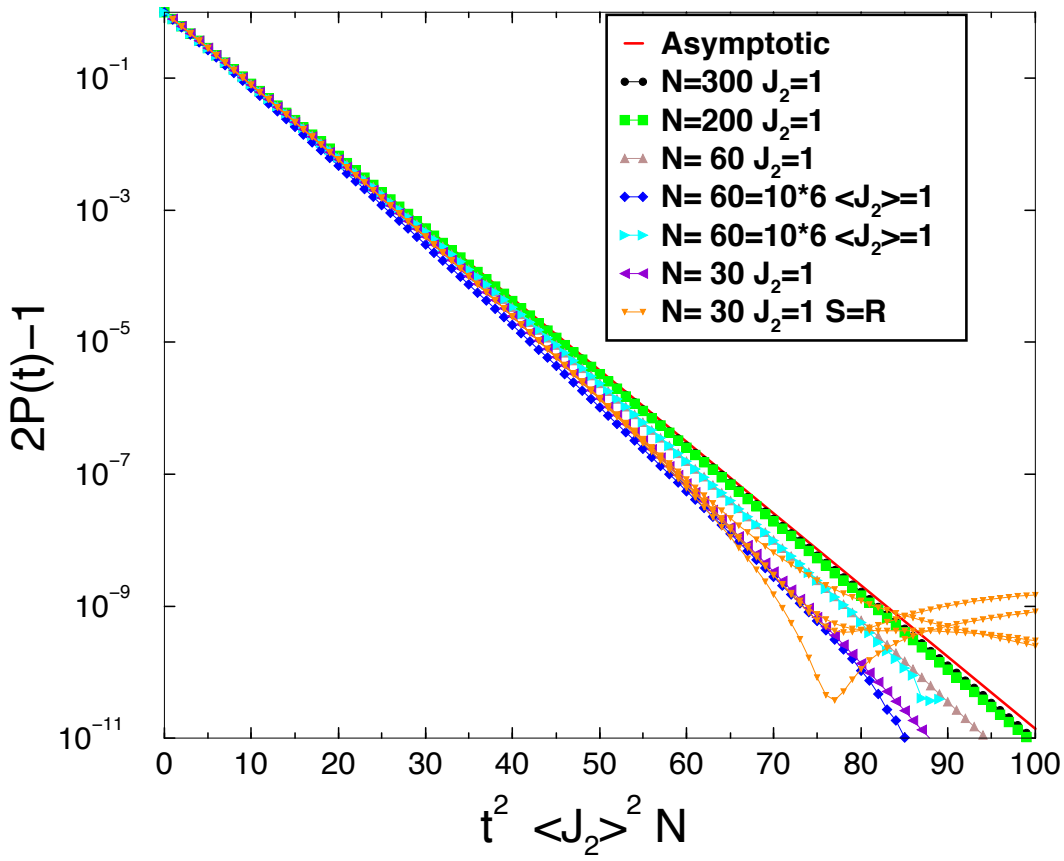

Figure 2. The quantity $2\mathcal{P}(t) - 1$ for the quantum purity $\mathcal{P}(t)$ is shown as a function of $t^2\langle J_2\rangle^2 N$; with $J_3 = 0$, $J_M = 0$ and $J_A = 0$. The asymptotic result is the solid red line from Eq. (43). Values for all $J_2 = 1$ are shown for $N = 30$, 60, 200, and 300 all starting with all spins down. For $N = 60$, as well as for 60 spins with $J_2 = 1$ [brown, $\triangle$], two different results are shown for $\langle J_2\rangle = 1$, but with ten baths each of six spins with the values [blue, $\diamond$, $J_2 = (1.5,\ 1.1,\ 1.03,\ 1.01,\ 1.001,\ 0.999,\ 0.99,\ 0.97,\ 0.9,\ 0.5)$] and [cyan, $\triangleright$, $J_2 = (1.01,\ 1.001,\ 1.0,\ 1.0,\ 1.0,\ 1.0,\ 1.0,\ 1.0,\ 0.999,\ 0.99)$]. For $N = 30$ five different random starting states for $|\Phi(0)\rangle$ are shown, all with $\alpha_0 = 0$ (orange), to compare with the other points which have all bath spins and the central spin intially down.

where the prime on the sum restricts the sum only to the terms that have the z-component of the magnetization of the bath spins equal to m_j. In the calculations performed in this paper, whenever a random state for the x-bath(s) is used, the c_j are chosen to be real and distributed uniformly between 0 and 1. After all the c_j are chosen randomly, the initial vector $\left|\widetilde{\Phi}(0)\right\rangle$ is normalized to unity. However, for large N the sum over so many random numbers is both time consuming and gives results that are subject to propagating round-off errors. Therefore, invoking the central limit theorem, the computer program was written so that when the number of terms in the primed sum of Eq. (45) was larger than 50 the sum was replaced by a random number drawn from a Gaussian distribution with the exact first and second moments expected from the sum over the squares of the required number of random terms.

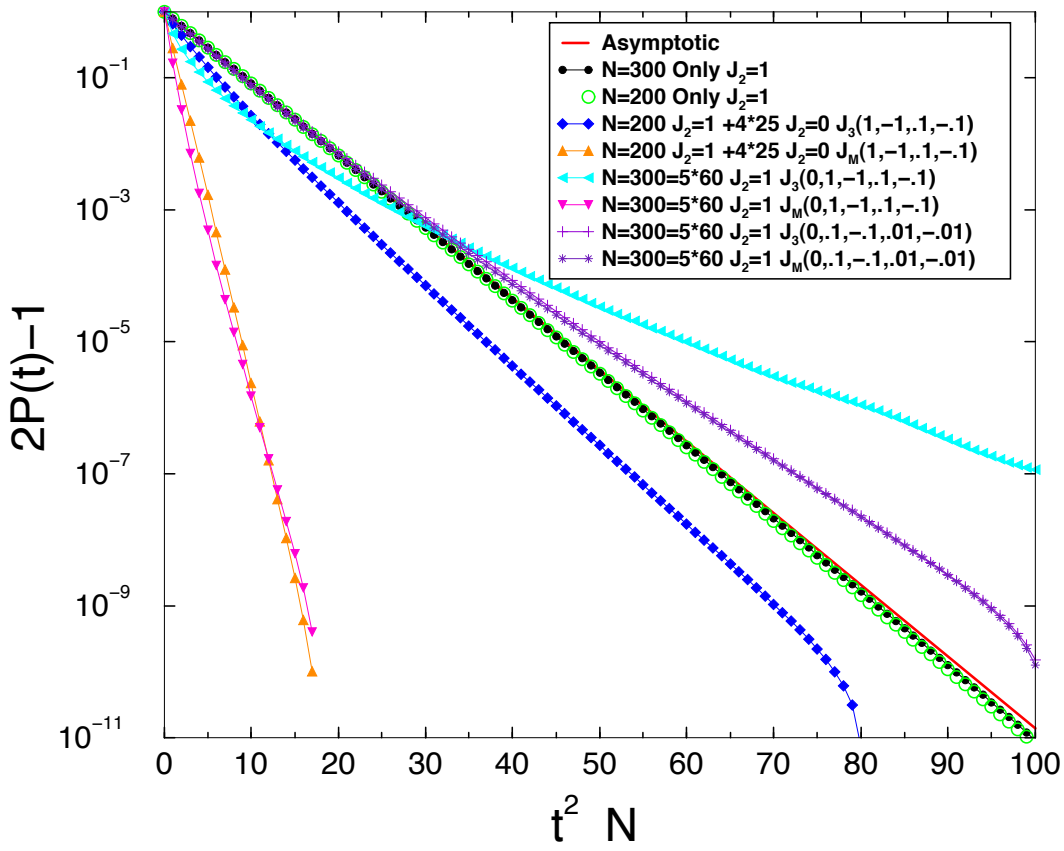

Figure 3. The quantity $2\mathcal{P}(t) - 1$ for the quantum purity $\mathcal{P}(t)$ is shown as a function of t^2N. The asymptotic result is the solid red line from Eq. (43). The starting state of all bath spins and the central spin is down. For $N = 300$ all baths have $J_2 = 1$. The $N = 300$ data (black, $\bullet$) is for one bath, and the others have five baths of 60 spins each with interactions [cyan, $\triangleleft$, $J_3 = (0, 1.0, 0.1, -0.1, -1.0)$], [magenta, $\bigtriangledown$, $J_M = (0, 1.0, 0.1, -0.1, -1.0)$], [violet, $+$, $J_3 = (0, 0.1, 0.01, -0.01, -0.1)$], and [indigo, $*$, $J_M = (0, 0.1, 0.01, -0.01, -0.1)$]. Also shown are results for five baths, one with only $J_2 = 1$ and 200 bath spins, and four baths of 25 spins each (so $N = 300$) with interactions [blue, $\diamond$, $J_3 = (1.0, 0.1, -0.1, -1.0)$] and [orange, $\bigtriangleup$, $J_M = (1.0, 0.1, -0.1, -1.0)$]. The case for $N = 200$ with only $J_2 = 1$ is also shown (green, $\bigcirc$).

5. Results and Analysis

We present test results to show that the algorithm does indeed work. One goal is to compare with the exact results of reference [16], and to extend these results for random J interactions, as well as for different starting vector configurations.

In Fig. 2 we show results for how the quantum purity $\mathcal{P}(t)$ approaches its asymptotic limit for the case where there is symmetry in the Hamiltonian under interchange of any two bath spins. The largest Hilbert space calculated in Fig. 2 is $2^{301} \approx 4 \times 10^{90}$. Clearly without the use of the algorithm in this paper and the symmetry of the Hamiltonian the calculations would be impossible. The largest number of 2×2 terms summed over in Fig. 2 is $7^{10} \approx 2.8 \times 10^8$ for the case of ten different x-baths. Fig. 2 shows that the quantum purity decays to its asymptotic $N \to \infty$ result of Eq. (43) even when the initial starting state is random or when there are a number of different x-baths with different couplings. In other words, in all cases except for finite

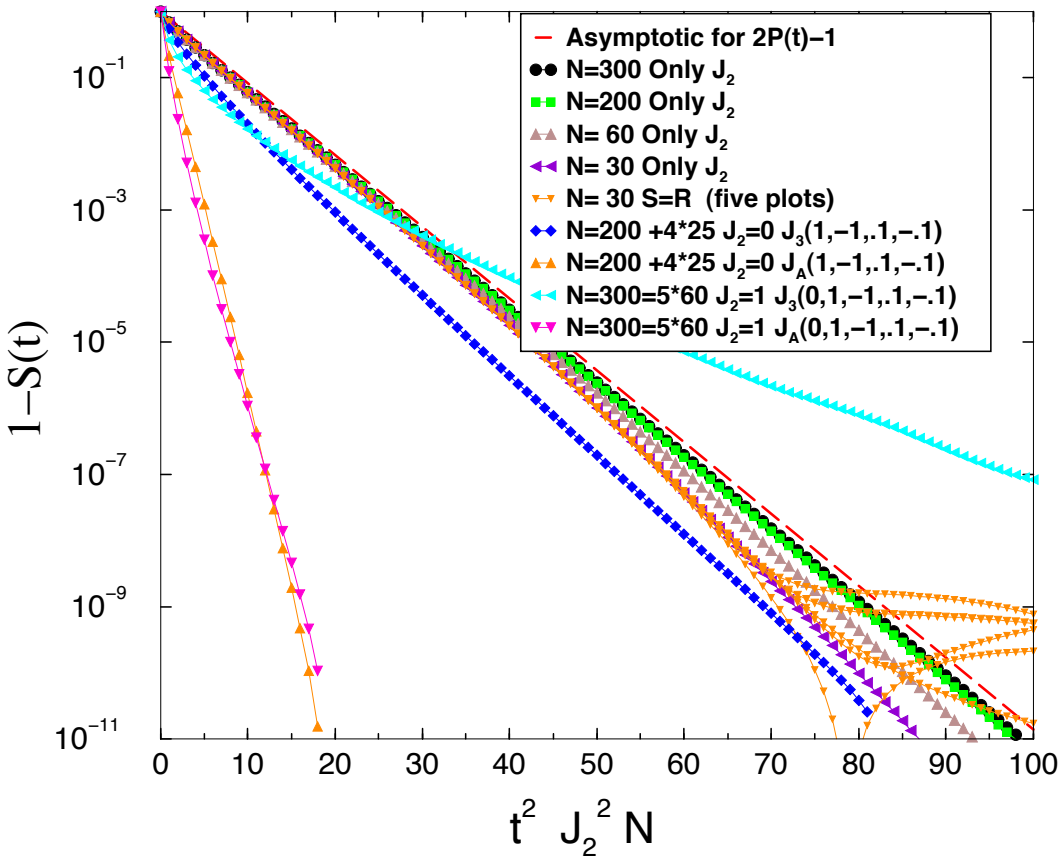

Figure 4. The von Neumann entropy $\mathcal{S}(t)$ subtracted from unity is shown as a function of $t^2\langle J_2\rangle^2 N$; with $J_3 = 0$, $J_M = 0$ and $J_A = 0$. The asymptotic result for $2\mathcal{P}(t) - 1$ is the dashed red line from Eq. (43), only to guide the eye. Values for all $J_2 = 1$ are shown for $N = 30$, 60, 200, and 300 all starting with all spins down. For $N = 30$ five different random starting states for $|\Phi(0)\rangle$ are shown, all with $\alpha_0 = 0$ (orange) [different random starting states than in Fig. 2]. The $N = 300$ data (black, $\bullet$) is for one bath, and the others have five baths of 60 spins with interactions [cyan, $\triangleleft$, $J_3 = (0, 1.0, 0.1, -0.1, -1.0)$] and [magenta, $\triangledown$, $J_M = (0, 1.0, 0.1, -0.1, -1.0)$]. Also shown are results for five baths, one with only $J_2 = 1$ and 200 bath spins, and four baths of 25 spins each (so $N = 300$) with interactions [blue, $\diamond$, $J_3 = (1.0, 0.1, -0.1, -1.0)$] and [orange, $\triangle$, $J_M = (1.0, 0.1, -0.1, -1.0)$]. Except for the $N = 30$ points labeled S=R (orange), all spins start down.

N effects and small effects due to the random starting state of the bath(s), the quantum purity decays exponentially in t^2 and N when the couplings are only 2-body between the bath(s) and the central spin.

In Fig. 3 the approach to the asymptotic value for the quantum purity $\mathcal{P}(t)$ is shown when the baths also may include the 3-body couplings with strength J_3 and N_i-body couplings J_A $(i = 1, \cdots, 5)$. Again, in all cases the decay of $\mathcal{P}(t)$ is exponential in t^2. The largest number of 2×2 matrices summed over in Fig. 3 is for five baths of 60 spins each, which requires $61^5 \approx 8\times10^8$ terms in the sum. Again, in all cases except for finite N effects, for large N the quantum purity decays exponentially in t^2 to its asymptotic value.

In Fig. 4 we show how the von Neumann quantum entropy $\mathcal{S}(t)$ approaches its asymptotic

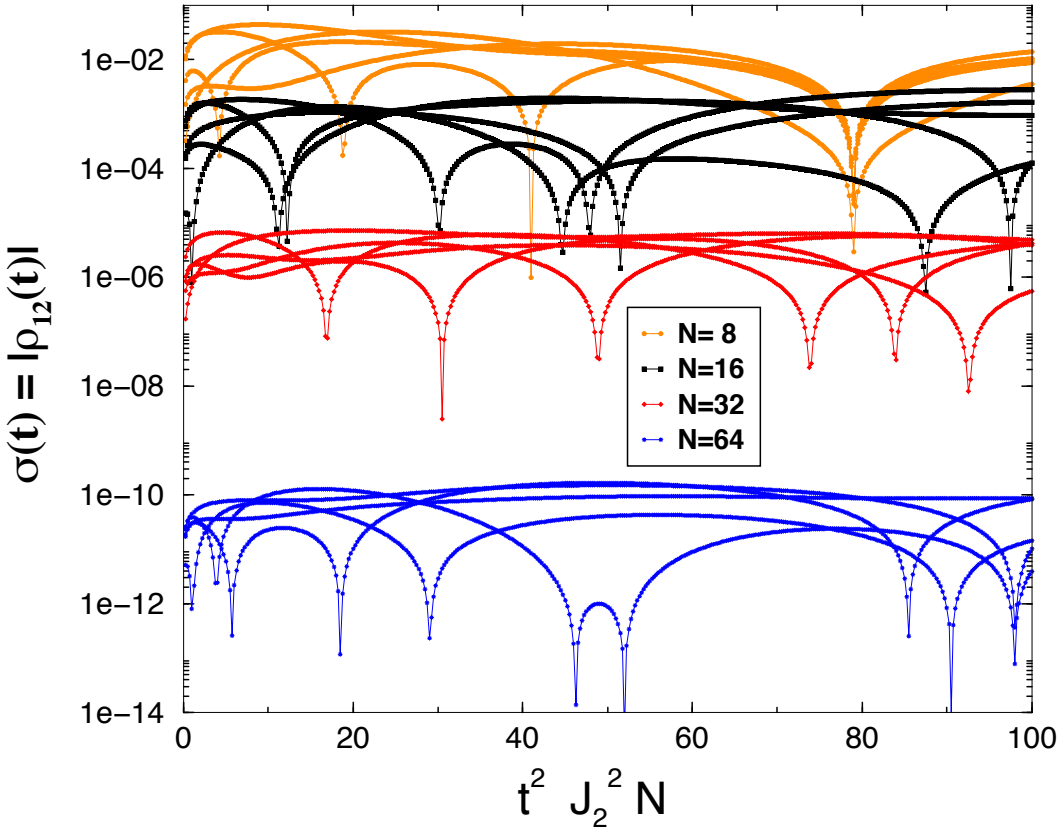

Figure 5. The quantity $\sigma(t) = |\rho_{12}(t)|$ is shown as a function of $NJ_2^2t^2$ for different values of N. The results are for random initial bath configurations $\left|\widetilde{\Phi}(0)\right\rangle$, and five different random states are shown for each value of N. The results are for one x-bath with only 2-body interactions of strength $J_2 = 1$.

value of unity. In all cases, except for finite N effects and small effects due to the random starting state of the bath(s), the quantum entropy decays exponentially in t^2. Comparing results for different baths of 300 spins in Fig. 3 and Fig. 4 shows that the interactions between the bath spins lead to quantitative but not qualitative differences in the behavior of $\mathcal{P}(t)$ and $\mathcal{S}(t)$.

In Fig. 5 we show the quantity $\sigma(t) = |\rho_{12}(t)|$ as a function of $NJ_2^2t^2$ for different values of N. A recent paper examined $\sigma(t)$ for a 4-spin cluster coupled to spin baths with up to $N = 32$ spins to study decoherence and thermalization [13]. The results shown in Fig. 5 are for the only non-zero couplings the 2-body coupling $J_2 = 1$. For an initial state of the bath with all spins down, the quantity $|\rho_{12}(t)|$ does not decay at all with t. Only for random initial states of the bath does $|\rho_{12}(t)|$ decay, and then it decays in an extremely short time and fluctuates about some average value. The average value of $|\rho_{12}(t)|$ decreases rapidly as N increases. The fact that $|\rho_{12}(t)|$ does not decay at all if all spins are started in the down (or the up) configuration illustrates the importance of a random initial state for the bath.

In Fig. 6 we examine one bath with only $J_2 = 1$ and an initial state for the bath with all spins up. The central spin is started at an angle α_0, as in Eq. (16). We see that the quantum purity no longer decays to zero if α_0 is not zero (or 90^o). Thus our x-bath does not act effectively for decoherence of all initial configurations of the central spin. This is a limitation of the x-baths.

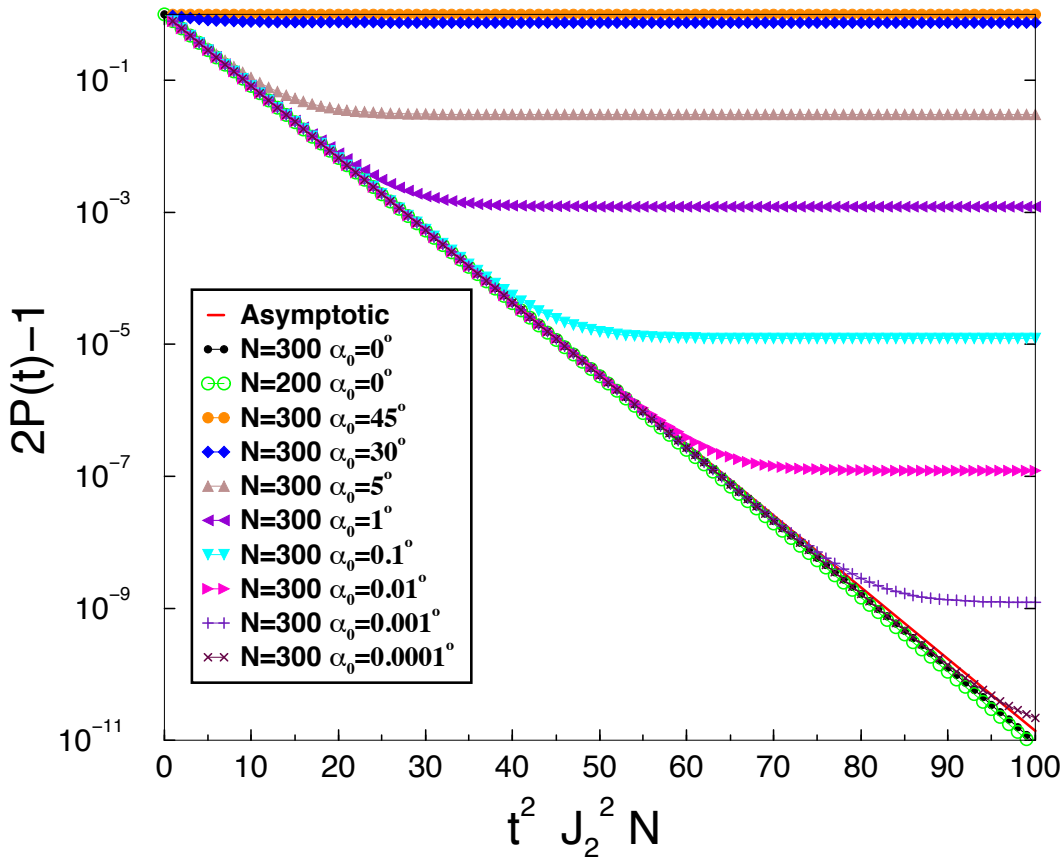

Figure 6. The quantity $2\mathcal{P}(t)-1$ for the quantum purity $\mathcal{P}(t)$ is shown as a function of $t^2J_2^2N$. The asymptotic result for $\alpha_0 = 0^o$ is the solid red line from Eq. (43). The starting state of all bath spins is down, and all $J_2 = 1$. For $N = 300$ the central spin has a starting state with different values of $\alpha_0 = 45^o$, 30^o, 5^o, 1^o, 0.1^o, 0.01^o, 0.001^o, and 0.0001^o. Also shown is $N = 200$ for $\alpha_0 = 0^o$.

In Fig. 7 we show the quantum purity (normalized and with its asymptotic value subtracted) $2\mathcal{P}(t) - 1$ as a function of the number of bath spins N times t^2. The coupling between the central spin and bath spins only has a coupling of the form $J_{2,i}S_0^xS_i^x$ with $J_{2,i}$ uniformly distributed in the range $[1-r, 1+r]$, and hence would qualify as an x-bath. However, here we do not limit ourselves to only x-baths, in that we allow intra-bath couplings of the form $\mathcal{H}_B = \sum_{i,j}^{N}\left(J_{ij}^xS_i^xS_j^x + J_{ij}^yS_i^yS_j^y + J_{ij}^zS_i^zS_j^z\right)$ with $J_{ij}^\ell \in [-r, +r]$ with $i = 1, \cdots, N$. Hence for $r = 0$ the results reduce to those of an x-bath, and hence are compared with Eq. (43) for asymptotic N and to a sum over only $N+1$ different terms in Eq. (24). Fig. 7 shows results for $N = 10$, 20, and 30. For non-zero r, we have used the Chebyshev algorithm of [12, 13] storing vectors of size 2^{N+1}. The asymptotic result is the dashed line from Eq. (43). In all cases even for this more general bath we find that the quantum purity decays exponentially in Nt^2, except for small finite-N and random coupling effects. The numerical results for zero disorder ($r = 0$) agree with our algorithmic results and the exact results of ref. [16]. Note in this case the $\mathcal{H}_B$ contains operators that do not commute with S^x, and therefore the bath has some internal dynamics. Even for the generalized bath and for the random interactions an exponential decoherence in t^2 is observed. Also note that for small values of r the results are closer to the asymptotic result

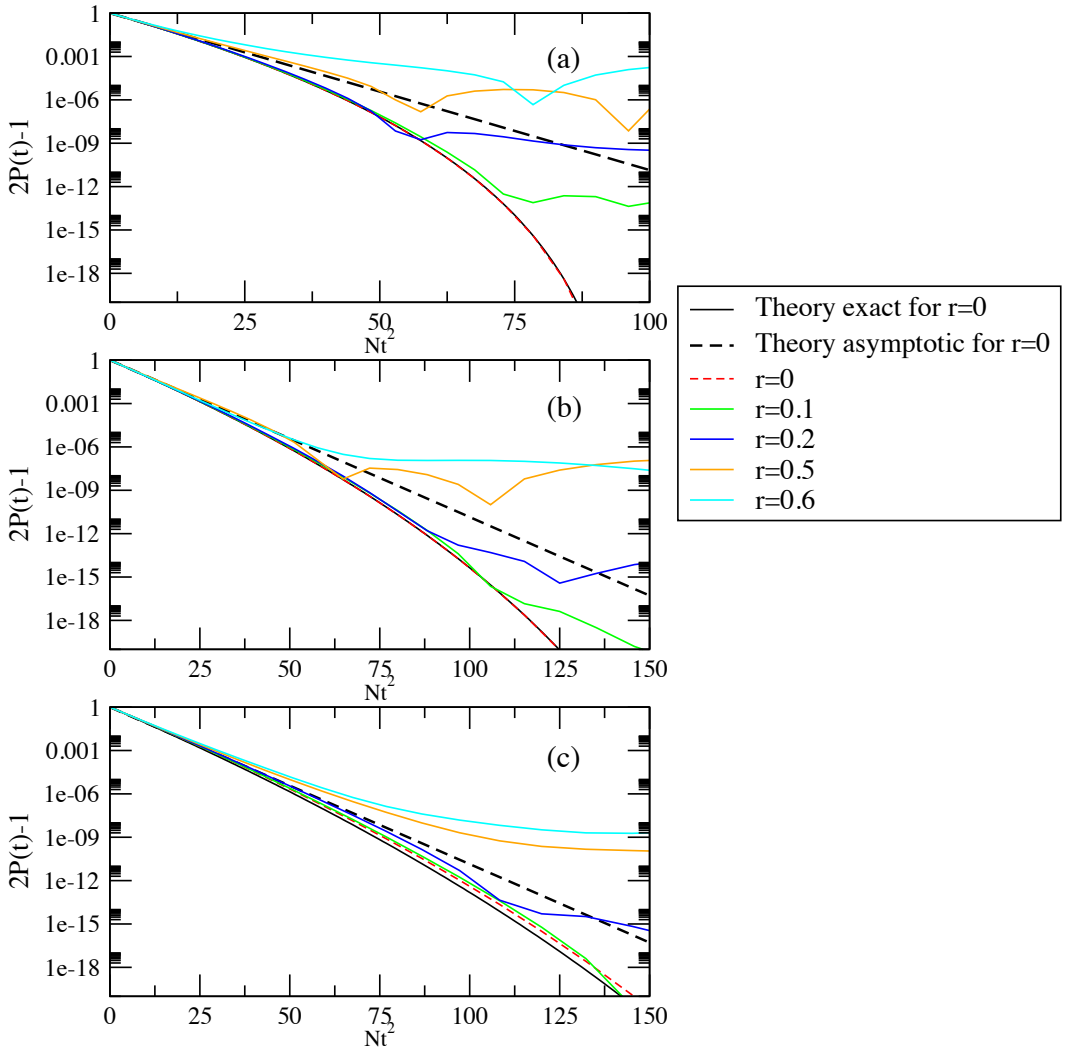

Figure 7. The quantity $2\mathcal{P}(t) - 1$ for the quantum purity $\mathcal{P}(t)$ is shown as a function of Nt^2 is shown for $J_i \in [1-r, 1+r]$ with $i = 1, \cdots, N$ and (a) $N = 10$, (b) $N = 20$, and (c) $N = 30$. The asymptotic result is the dashed line from Eq. (43). Note, the bath is only an x-bath for $r = 0$. This figure is related to that of reference [17].

than for the case with $r = 0$.

6. Conclusions and Discussion

We have shown that for a single spin coupled to specific types of spin baths, which we denote as x-baths, an efficient algorithm can be devised that eliminates the computer storage of large vectors. The x-baths are those that have in the Hamiltonian only the operators S_k^x $(k = 1, \cdots, N)$. Since we are not interested in the dynamics of the bath spins, we trace out the bath spins to obtain the reduced density matrix $\rho(t)$ of the central spin(s). To obtain the real-time propagation using the time dependent Schrödinger equation (TDSE) of a central spin coupled to N bath spins, one would normally be required to store one or more vectors of size the dimension of the Hilbert space, 2^{N+1}. We find that the dynamics of x-baths is such that the intra-bath Hamiltonian $\mathcal{H}_B$ does not affect the dynamics of the central system. For the x-baths with a single central spin,

no vectors of dimension larger than 2 must be stored. Furthermore, from Eq. (24) the density matrix $\rho(t)$ of the central system is a sum over 2^N density matrices $\rho_j(t)$ that each have their own Hamiltonian. Once $\rho(t)$ has been obtained, in the normal fashion using Eq. (26) expectation values of operators can be calculated. An example for $\langle S_0^z(t)\rangle$ is shown in Fig. 1.

The algorithm requires that one solves the TDSE for 2^N different Hamiltonians of the size of the subsystem studied. In this paper the subsystem studied is a single spin, so the TDSE propagation of 2^N vectors of length 2 is required. Symmetries in the Hamiltonian can be used to further reduce the number of different TDSE Hamiltonians that one needs to sum to obtain $\rho(t)$. The reduction in the number of different terms in the sum for $\rho(t)$ only requires symmetry in the spin-bath Hamiltonian $\mathcal{H}_{SB}$, not in the initial vector of the bath (provided that the central spin is brought into contact with the bath at $t = 0$). The largest Hilbert space calculated in this paper is $2^{301} \approx 4 \times 10^{90}$, for one central spin and a bath of $N = 300$. For this type of bath, which has maximum symmetry in the bath, the number of different Hamiltonians one needs to propagate with the TDSE is only $N + 1$. Clearly without the use of the algorithm in this paper, and the symmetry of the Hamiltonian, the calculations performed in this paper would be impossible. If there is less symmetry in the bath, a smaller reduction in the number of different terms needed in the sum for $\rho(t)$ are obtained. For example, in Fig. 2 with $N = 60$ there are data points with ten symmetric baths with six spins each. For these points the Hilbert space is $2^{61} \approx 2 \times 10^{18}$ but results for $\rho(t)$ is from the sum of $7^{10} \approx 2.8 \times 10^8$ different 2×2 terms $\rho_j(t)$.

We used this algorithm to study a single spin coupled to different types of x-baths. If the central spin is either up or down initially, the quantum purity $\mathcal{P}(t) = \mathrm{Tr}\left[\rho^2(t)\right]$ decays exponentially in t^2 times N to its asymptotic value, as seen in Fig. 2 and Fig. 3. Furthermore, in this case the von Neumann entropy $\mathcal{S}(t)$ decays to its asymptotic value exponentially in t^2 and N as seen in Fig. 4. In addition, if the initial vector(s) of the spins in the bath(s) is (are) random, the off-diagonal component of the density matrix for a single spin in the central system $|\rho_{12}(t)|$ decreases with N as seen in Fig. 5. These exponential approaches to the asymptotic $N \to \infty$ limit are very good for finite N values up to a particular time t, where the size of the bath and the starting state of the bath becomes important (see Fig. 2, Fig. 3, and Fig. 4).

Unfortunately, the x-baths are not sufficient to always provide adequate decoherence and thermalization of the central system. This is seen in one instance in that $|\rho_{12}(t)|$ is time independent if the initial state of the bath is the state with all spins down or all spins up. The lack of ability of the x-baths to cause full decoherence of the central system is also illustrated in Fig. 6. Fig. 6 illustrates that if the central spin is not initially in either the up or down state the quantum purity $\mathcal{P}(t)$ saturates to a finite value. We have also used a Chebyshev algorithm [12, 13] for the more general case where the spin-bath Hamiltonian only has couplings of the form of an x-bath, namely $\mathcal{H}_{SB} = \sum_{i=1}^{N} J_i^x S_0^x S_i^x$, but the bath Hamiltonian $\mathcal{H}_B$ has general random two-body couplings with the operators $S_i^x S_j^x$, $S_i^y S_j^y$, and $S_i^z S_j^z$. As seen in Fig. 7 the approach of $\mathcal{P}(t)$ to its asymptotic values is still exponential in t^2 and N. The bath in Fig. 7 has its own internal dynamics even when it is not coupled to the central spin(s), and therefore should allow for decoherence and thermalization of the central spin(s) for all initial spin configurations.

Our x-bath algorithm can be expanded in several different directions. One is to also allow simultaneously x-baths, y-baths, and z-baths. The x-baths have only terms in the Hamiltonian using the operators S_k^x. Similarly the y-baths (z-baths) would only have terms in the Hamiltonian using the operators S_k^y (S_k^z). It has recently been shown that for a single central spin coupled to both an x-bath and a y-bath, the approach of the quantum purity $\mathcal{P}(t)$ to its asymptotic value becomes a power law in t and N [16]. This contrasts with the exponential dependence in t^2 and N for only an x-bath. A physically interesting question that can be studied with the expanded algorithm is under which circumstances the approach to the asymptotic value for the quantum purity and von Neumann entropy is power law or is exponential for different

combinations of x-, y-, and z-baths [18]. For y-baths one could use

$$p_y = \frac{1}{\sqrt{2}} \begin{pmatrix} -i & i \\ 1 & 1 \end{pmatrix} , \tag{46}$$

which has the same properties as p_x of Eq. (10) for x-baths. Another direction of improving the algorithm would be to apply it to a larger number of spins in the central system. If there were M spin-1/2 particles in the central system, the calculation of the density matrix would reduce solving the TDSE for 2^N Hamiltonians that have a Hilbert space of size 2^M. Such calculations could be accomplished even for the case where the central subsystem Hamiltonian $\mathcal{H}_S$ is time dependent as long as the $2^M \times 2^M$ matrix can be propagated efficiently via the TDSE.

Our efficient algorithm for solving the TDSE for central spins coupled to x-bath spins should pave the way for other efficient algorithms for the real-time development of spin systems. Such algorithms would allow one to study quantum decoherence, thermalization of quantum systems coupled to spin baths, and may be applicable to applications such as quantum encryption and quantum computing.

Acknowledgements
This material is based upon work supported in part for MAN by the US National Science Foundation under Grant No. DMR-1206233. MAN also acknowledges support from the Jülich Supercomputing Centre (JSC).

References

[1] Mermin D.N., *Quantum Computer Science: An Introduction* (Cambridge University Press, Cambridge, UK, 2007).
[2] Kaye P., Laflamme R., Mosca M., *An Introduction to Quantum Computing* (Oxford University Press, Oxford, UK, 2007).
[3] Shankar R., *Principles of Quantum Mechanics*, Second Edition (Plenum Press, London, 1994).
[4] Fermi E., 1932 *Rev. Mod. Phys.* **4**, 87.
[5] Prokof'ev N.V. and Stamp P.C.E., 2000 *Rep. Prog. Phys.* **63**, 669.
[6] Yang W. and Liu R.-B., 2009 *Phys. Rev. B* **79**, 115320.
[7] Xu J., Jing J., and Yu T., 2011 *J. Phys. A: Math. and Theor.* **44**, 185304.
[8] http://www.top500.org.
[9] Tal-Ezer H., and Kosloff R., 1984 *J. Chem. Phys.* **81**, 3967.
[10] Leforestier C., Bisseling R., Cerjan C., Feit M., Friesner R., Guldberg A., Hammerich A., Jolicard G., Karrlein W., Meyer H.-D., Lipkin N., Roncero O., and KosloffR ., 1991 *J. Comput. Phys.* **94**, 59.
[11] Iitaka T., Nomura S., Hirayama H., Zhao X., Aoyagi Y., and Sugano T., 1997 *Phys. Rev. E* **56**, 1222.
[12] Dobrovitski V.V., and De Raedt H., 2003 *Phys. Rev. E* **67**, 056702.
[13] Jin F., De Raedt H., Yuan S., Katsnelson M.I., Miyashita S., and Michielsen K., 2010 *J. Phys. Soc. Japan* **79**, 123005.
[14] Danon J., Vink I.T., Koppens F.H.L., Nowack K.C., Vandersypen L.M.K., and Nazarov Y.V., 2009 *Phys. Rev. Lett.* **103**, 046601.
[15] Vink I.T., Nowack K.C., Koppens F.H.L, Danon J., Nazarov Y.V., and Vandersypen L.M.K., 2009 *Nature Physics* **5**, 764.
[16] Rao D.D.B., Kohler H., and Sols F, 2008 *New J. Physics* **10**, 115017.
[17] Guerra M.L., De Raedt H., and Novotny M.A., 2011 *Physics Procedia* **15**, 33.
[18] Novotny, M.A., Guerra, M.L., De Raedt H., Michielsen, K., and Jin, F., 2012 *Physics Procedia* **34**, 90.